


ORIGINAL ARTICLE

Distinct clinicopathological features of pulmonary primary angiomatoid fibrous histiocytoma: A report of four new cases and review of the literature

Zheng Wang^{1†}, Liping Zhang^{2†}, Li Ren³, Dongge Liu¹ , Jun Du¹, Min Zhang⁴, Ge Lou⁵, Ying Song⁶, Yin Wang⁶, Chunyan Wu² & Guiping Han⁵

1 Department of Pathology, Beijing Hospital, National Center of Gerontology, Institute of Geriatric Medicine, Chinese Academy of Medical Sciences, Beijing, China

2 Department of Pathology, Shanghai Pulmonary Hospital, School of Medicine, Tongji University, Shanghai, China

3 Department of Pathology, Air Force Medical Center of PLA, Beijing, China

4 Department of Radiology, Beijing Hospital, National Center of Gerontology, Institute of Geriatric Medicine, Chinese Academy of Medical Sciences, Beijing, China

5 Department of Pathology, the Second Affiliated Hospital of Harbin Medical University, Harbin, China

6 Berry Oncology Corporation, Fuzhou, China

Keywords

Differential diagnosis; *EWSR1* gene fusion; histological change; metastasis; pulmonary primary angiomatoid fibrous histiocytoma.

Correspondence

Guiping Han, Department of Pathology, the Second Affiliated Hospital of Harbin Medical University, No.246, Xuefu Road, Nangang District, Harbin, Heilongjiang Province 150086, China.
Tel: +86 451 8629 6970
Fax: + 86 451 8629 6612
Email: gphancn@163.com

Chunyan Wu, Department of Pathology, Shanghai Pulmonary Hospital, School of Medicine, Tongji University, Shanghai 200433, China.
Tel: +86 18017729697
Fax: +86 21 6511 5006
Email: wuchunyan581@163.com

Dongge Liu, Department of Pathology, Beijing Hospital, National Center of Gerontology, Institute of Geriatric Medicine, Chinese Academy of Medical Sciences, 1 Dahua Rd, Dongcheng District, Beijing 100730, China.
Tel: +86 10 8513 3885
Fax: +86 10 8513 3885
Email: 13661275182@163.com

[†]Zheng Wang and Liping Zhang contributed equally.

Received: 14 September 2020;

Accepted: 16 October 2020.

doi: 10.1111/1759-7714.13727

Abstract

Background: The aim of this study was to highlight the clinicopathological features of pulmonary primary angiomatoid fibrous histiocytoma (PPAFH) to assist with a differential diagnosis.

Methods: There were 10 previous reports in the literature and four new PPAFH cases reviewed in this study. Immunohistochemistry (IHC), fluorescence in situ hybridization (FISH) and DNA and RNA-based next-generation sequencing (NGS) was performed in the four new cases reported here.

Results: In the four new PPAFH cases, the ages of occurrence were in patients age from 33 to 55 years and tumor sizes were from 1.5 to 8 cm. Three of four (75.0%) tumors were located in the endobronchus. The most common morphological changes included delineated fibrous capsule (100%, 4/4), lymphoplasmacytic cuff (100%, 4/4), and dense or richly lymphoplasmatic infiltration (100%, 4/4). IHC analysis revealed that the tumor cells of four cases expressed vimentin and TLE1, ALK and CD163 or CD68 was positive in three cases, epithelial membrane antigen (EMA), desmin was positive in two cases, and SMA focal positive expression was observed in two cases. *EWSR1* gene rearrangement was positive in all PPAFH cases (100%, 4/4) by FISH detections and four cases were confirmed as *EWSR1-CREB1* fusion variant by DNA and RNA based NGS. No regional lymph nodes and distal metastasis, recurrences and death of disease after surgical excision were recorded in all four cases.

Conclusions: PPAFH is a very unusual pulmonary primary mesenchymal tumor and the clinicopathological features are like other unusual sites counterparts, but with a smaller tumor size, related with large airway, with a tendency to exhibit benign biological behavior, with *EWSR1* gene rearrangement and higher frequency of *EWSR1-CREB1* gene fusion.

Key points

Significant findings in the study

In comparison with “classic somatic” and nonpulmonary visceral angiomatoid fibrous histiocytoma, pulmonary primary angiomatoid fibrous histiocytoma display distinct clinicopathological features and prognosis.

What this study adds

The study provided the pathological differential diagnostic criteria and clinicopathological features for pulmonary primary angiomatoid fibrous histiocytoma.

Introduction

Angiomatoid fibrous histiocytoma (AFH) is a rare soft tissue tumor with low frequency recurrence, with metastasis first reported in 1979 by Enzinger.¹ Apart from the so-called “classic somatic” AFH, the “unusual sites” counterparts have been previously reported in the lung, mediastinum, vulva, retroperitoneum, ovary and pulmonary artery, bone, intracranial lesions, etc.^{2–6}

To date, 10 pulmonary primary AFH (PPAFH) have been reported in English studies, the first case being introduced by Ren *et al.* in 2009.⁷ The differences in clinicohistological features among somatic, nonpulmonary unusual sites and PPAFH, especially long-term prognosis of PPAFH, have not yet been fully discussed. The morphological features and molecular alternations of PPAFH overlap with a wide spectrum of pulmonary mesenchymal neoplasms, including inflammatory myofibroblastic tumors (IMTs), primary pulmonary myxoid sarcoma (PPMS) with *EWSR1* rearrangement, and follicular dendritic cell sarcoma (FDC), etc. It remains problematic for clinicians to determine a precise differential diagnosis for patients with PPAFH.^{8–13} The four new PPAFH cases collected here, together with the 10 literature reports, were included in the study with the aim of determining the clinicopathological characteristics and definite differential diagnosis criteria for PPAFH.

Methods

Case selection

The four PPAFH cases were collected from three Chinese medical centers (one from Second Hospital Affiliated Harbin Medical University, one from Beijing Hospital and two from Shanghai Pulmonary Hospital) from 2017 to 2019. Clinical data and radiological images were obtained. Histological slides were reviewed by four pulmonary pathologists (ZW, LPZ, CYW and GPH). All of the four patients signed their informed consent to be included in this study.

Immunohistochemistry

IHC staining was performed on 4 μ m thick formalin-fixed paraffin embedded (FFPE) sections from four PPAFH current cases. Antibodies including cytokeratin, vimentin, EMA, CD68 or CD163, desmin, SMA, CD34, S-100, CD21,

CD35, CD99, CD31, Ki-67 were used for IHC staining. Slides were stained on Autostainer Link 48 platform (Agilent Technologies, Santa Clara, CA). Ventana ALK (D5F3) kit was used to test ALK protein expression (Ventana Medical Systems, Inc., Tucson, AZ, USA), in accordance with the manufacturer's instructions, which was performed automatically using the Ventana Benchmark XT Stainer (Ventana Medical Systems Inc., Tucson, AZ, USA).

Fluorescence in situ hybridization (FISH)

ALK and *EWSR1* gene translocation and copy number variation was detected on 4 μ m thickness FFPE sections by FISH using dual-colored break-apart probes (HealthCare Biotechnology Co., Ltd. Wuhan, China). The manufacturer's protocol of *ALK* and *EWSR1* gene FISH break-apart probe kit was followed during FISH hybridization procedures, respectively. Interpretation of positive cases were defined as those presenting split signals (the 5'-part [green fluorescence] and 3'-part [red fluorescence] signals were regarded as split when the separation distance was greater than two fluorescence signal diameters) or there was an isolated red signal in more than 10% of tumor cells. Meanwhile *ALK* gene copy number variation (CNVs) of each case was recorded. Amplification of *ALK* gene was defined as the presence of ≥ 6 copies of *ALK* per cell in $\geq 10\%$ of analyzed cells.¹⁴

DNA and RNA level next-generation sequencing (NGS)

Tumor DNA and RNA were coextracted from FFPE samples. Cancer mutation profiling was performed using the commercial Solid Tumor Comprehensive Test assay, which is a liquid hybridization-based target-enriched NGS method including a 654-gene DNA panel and a 105-gene RNA panel (provided by Berry Oncology Co., Ltd.). Libraries were sequenced using Illumina Novaseq 6000 system (Illumina, Inc., San Diego, California, USA) in 150 PE mode. Sequencing data was base-called, demultiplexed and filtered.¹⁵ Adapter sequences were trimmed and the reads were mapped to hg19.¹⁶ Mapped reads were deduplicated and the consensus reads were used for somatic variant calling.

Table 1 Clinicopathological findings of 14 pulmonary primary angiomatoid fibrous histiocytoma cases (four current cases and 10 literature cases)

| Sex/Age (years) | Surgery/location | Size/grossly | Fibrous capsule | Lymphoplasmatic infiltrate | Polymorphic/mitosis | Myxoid stroma | Angio-feature | Bronchial component | Follow-up months | References |
|-----------------|---------------------|--------------------------------------|----------------------|------------------------------------|---------------------|---------------------|---------------|---------------------|-------------------|----------------------|
| 1(C) Male/50 | Wedge Res/LLL | 20 mm/ endobronchial mass | Delineated | Peritumoral band/dense intertumor | Focal/rare | Focal | No | present | 22 months/ / | / |
| 2(C) Female/33 | Lobectomy/RML | 80 mm/W.D., cystic-solid, hemorrhage | Partially surrounded | Peritumoral band/dense intertumor | Focal/rare | Focal | Present | No | 17 months/ / | / |
| 3(C) Female/55 | Lobectomy/LUL | 15 mm/ endobronchial mass | Partially surrounded | Peritumoral band/dense intertumor | Focal/rare | No | No | Present | 13 months/ / | / |
| 4(C) Male/35 | Lobectomy/RLL | 15 mm/ endobronchial mass | Partially surrounded | Peritumoral band/ricily intertumor | Focal/1-2/10HPFs | 30% of entire tumor | No | Present | 30 months/ / | / |
| 1(L) Male/49 | Lobectomy/RLL | 21 mm/W.D., yellow-tan | Delineated | Peritumoral band/dense intertumor | Focal/rare | Present | NA | Present | 150 months/ N.R.# | Ren et al. (2009) |
| 2(L) Male/46 | Excision/RLL | 25 mm/W.D., grayish-yellow | Partially surrounded | Peritumoral band/ricily intertumor | No/rare | Present | NA | NA | 24 months/ / | Chen, et al. (2012) |
| 3(L) Female/60 | Excision/LUL | 15 mm/W.D., grayish-yellow | Partially surrounded | Peritumoral band/ricily intertumor | No/rare | Present | Present | NA | 17 months/ / | Chen, et al. (2012) |
| 4(L) Male/43 | Excision/lung | 24 mm/W.D., grayish-yellow | Partially surrounded | Peritumoral band/ricily intertumor | No/rare | Present | NA | NA | NA | Chen, et al. (2012) |
| 5(L) Male/64 | Lobectomy/LLL | 15 mm/ endobronchial mass | Partially surrounded | Peritumoral band/dense intertumor | No/No | NA | No | Present | NA | Thway, et al. (2012) |
| 6(L) Male/61 | S.R/RMB | 15 mm/ endobronchial mass | Partially surrounded | No/ricily intertumor | No/up to 3/10HPFs | Focal | No | Present | NA | Thway, et al. (2012) |
| 7(L) Male/27 | S.R/ endotracheal | 15 mm/endotracheal polypoid mass | NA | Peritumoral band/ricily intertumor | Focal/1-2/10HPFs | obvious | Present | Present | NA | Chen, et al. (2013) |
| 8(L) Female/70 | Wedge + LIN Res/RUL | 13 mm/W.D. mass, tan-white | Partially surrounded | NA/dense intertumor | No/rare | NA | No | NA | NA* | Tay, et al. (2016) |
| 9(L) NA/NA | NA | NA/NA | NA | Peritumoral band/ricily intertumor | NA | NA | NA | NA | NA | Cheah, et al. (2019) |
| 10(L) Female/22 | HBSR/ endotracheal | 15 mm/ endotracheal polypoid mass | Present | Peritumoral band/NA intertumor | NA | NA | NA | Present | 36 months/ / | Bouma, et al. (2019) |

C, current case; L, literature case; W.D., well demarcated mass; Res, resection; LLL & LUL & RML & RUL & RMB (L, left; R, right; LL, lower lobe; UL, upper lobe; ML, middle lobe; MB, main bronchus); HBSR, hybrid bronchoscopic and surgical resection; NA, not available data; No, no present; N.R., no recurrence; #, Literature Case 1 was followed-up by phone call in this study and there was no evidence of recurrence or metastasis after resection of the right lower lobe of lung (150 months).

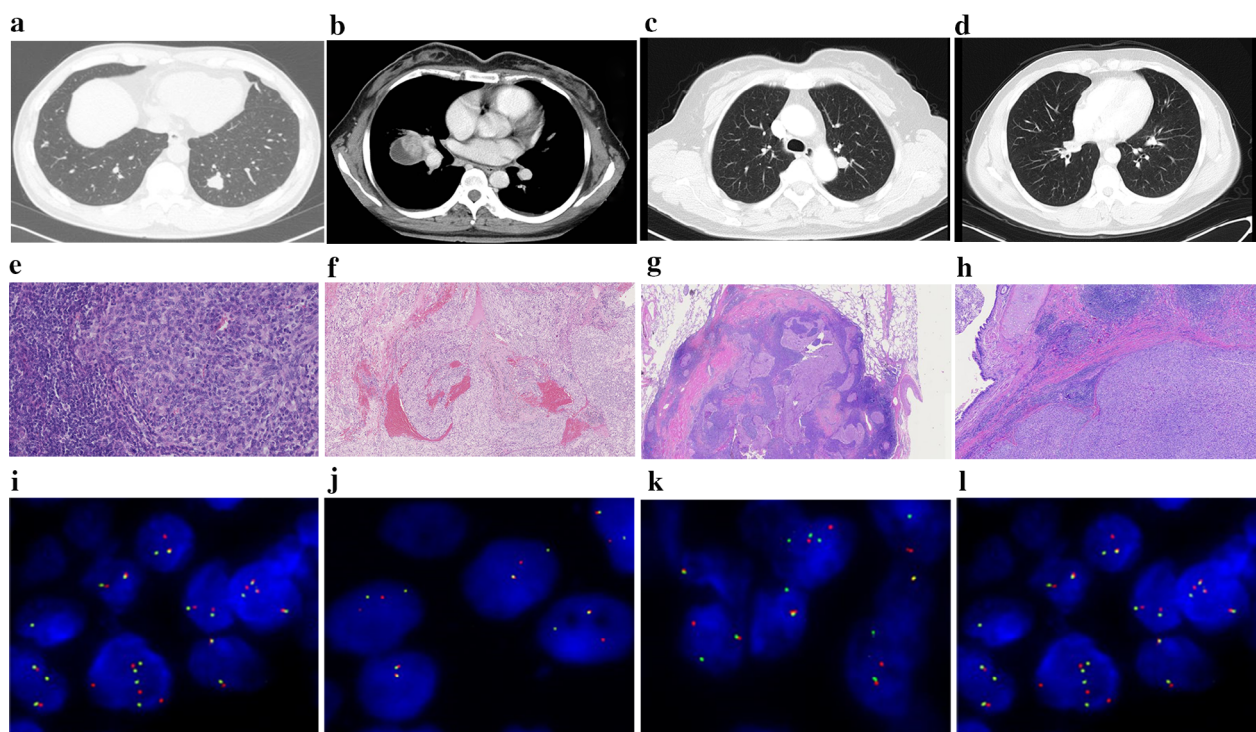


Figure 1 (a, c, d) Lung window of chest computed tomography (CT) of the current cases 1, 3, 4. (b) Mediastinal window in venous phase of contrast-enhanced chest CT of the current Case 2. The four lesions presented as clear boundary tumor. An endosubbronchial nodule in the posterior basal segment of left lower lobe, shallow lobulated (a, current Case 1). Right hilar mass with solid and cystic components, the hypoenhancing cystic part represents the bleeding (b, current Case 2). An endobronchial nodule in the apical subsegment of left upper lobe (c, current Case 3). An endobronchial nodule in the medial basal segment of the right lower lobe (d, current Case 4). (e–h) Histological features of the current Cases 1 to 4 with H&E staining. Tumor (current Case 1) showing coalescent pale-staining nodule with interspersed lymphoid and plasma cells (e) (H&E $\times 100$). The tumor of current Case 2 showing neoplastic cells arranged in closely packed nodules or sheet pattern with blood-filled pseudoangiomatous spaces (f) (H&E $\times 100$). The low power microscopic appearance of current Cases 3 and 4 displaying the endobronchial location, delineated fibrous capsule, lymphoplasmacytic cuff and dense lymphoplasmatic infiltration (g, h) (H&E $\times 10$ and $\times 40$). (i–l) Fluorescence in situ hybridization using break-apart probes for the *EWSR1* gene rearrangement of the current Cases 1–4. All of the four cases showing the separate red and green signals or single red signal in the nucleus and showing the presence of *EWSR1* gene translocation.

Results

Clinical findings

The clinical features of the four new PPAFH cases are summarized in Table 1. Case 1 (male/50 years) attended the hospital with a persistent cough and sputum production. Case 2 (female/33 years) had suffered from pulmonary tuberculosis (TB) for 22 years and developed symptoms of cough and hemoptysis, and then a solid and cystic mass was detected in the right hilum following CT scanning. In Case 3 (female/55 years) and Case 4 (male/35 years) an endobronchial mass was incidentally found during physical checkup. No smoking or any occupational exposure history were recorded in the four cases. Chest CT confirmed that the patients had four lesions which were clear boundary tumors. There were nodules within the endobronchus in Cases 1, 3 and 4 and

Table 2 Details of the fusion variants detected by next-generation sequencing (NGS) assay in the four current cases

| Sample No. | Fusion type (exons) | Breakpoint at 5' partner | Breakpoint at 3' partner |
|----------------|-----------------------------|--------------------------|--------------------------|
| Current Case 1 | <i>EWSR1-CREB1</i> (E7; C7) | chr22: g.29683842 | chr2: g.208437029 |
| Current Case 2 | <i>EWSR1-CREB1</i> (E8; C7) | chr22: g.29684775 | chr2: g.208436187 |
| Current Case 3 | <i>EWSR1-CREB1</i> (E7; C7) | chr22: g.29683648 | chr2: g.208435968 |
| Current Case 4 | <i>EWSR1-CREB1</i> (E7; C6) | chr22: g.29683977 | chr2: g.208435010 |

Case 2 had a right hilar peribronchial mass (Fig 1a–d). All four lesions were completely excised via wedge resection (Case 1) or lobectomy (Case 2, 3, 4) without any adjuvant therapy.

Pathological findings

The pathological characteristics of the four PPAFH cases are summarized in Table 1. Grossly, Cases 1, 3, and 4 presented with a nodule located in the endobronchus, and Case 4 was

found to have a peribronchial mass. All of the tumors were well-circumscribed and the tumor sizes of Cases 1–4 were 2.0, 8.0, 1.5, and 1.5 cm, respectively. All of the nodules cut surfaces presented as solitary, yellow-tan or white-tan, solid, firm with hemorrhagic foci, but there was cystic changes and extensive hemorrhage evident in Case 2.

Microscopically, all of the four PPAFH cases had delineated or partial hyaline fibrous capsule, lymphoplasmacytic cuff and dense or richly lymphoplasmatic infiltration. Pseudoangiomatous spaces were present in Case 2. The tumor cells were multiple coalescent, island nodules, packed solid, or sheet arrangement, and predominantly spindle, short spindle, and epithelioid, histiocytoid tumor cell morphological changes or patchy clear cell (Case 4). Focal pleomorphic nuclei could be seen in all four cases. Mitoses were presented up to 1–2/10 HPF in Case 4. No necrosis was identified in all four cases. The stroma of tumor presented as focal (Case 1, 2) to obvious myxoid change (Case 4) with reticular pattern, focal sclerotic stroma (current Cases 1, 3, 4) and hemorrhage (current Case 2) (Fig 1e–h).

Immunohistochemical and genetic findings

The tumor cells of four cases expressed vimentin and TLE1. Three of four cases presented CD68 or CD163 staining positive (Cases 1, 2, 3), two cases expressed EMA (Cases 3, 4), SMA (Cases 1, 3, focally), and desmin (Cases 2, 3). Tumor cells were completely negative for cytokeratin (AE1/AE3), dendritic cell markers (CD21, CD23, CD35), CD34, CD31, S100. ALK protein expression was observed in three cases (Cases 1, 3, 4) by Ventana ALK (D5F3) kit. The Ki-67 labeling index

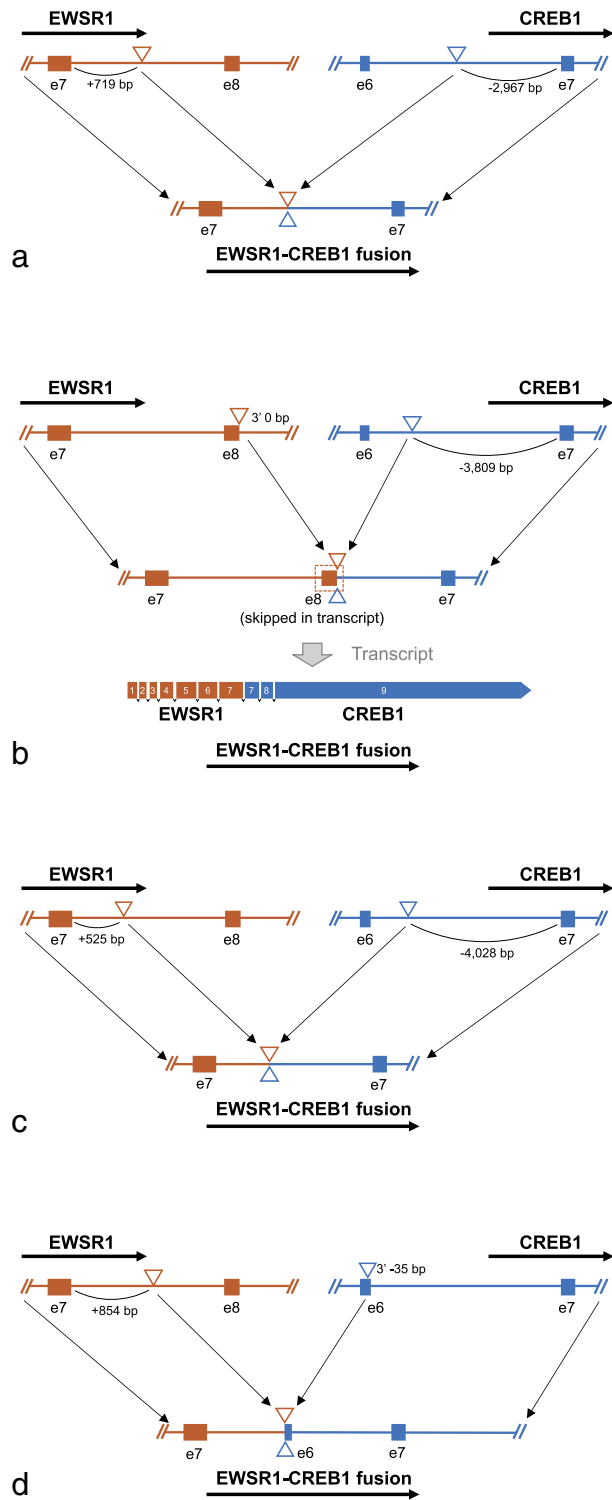


Figure 2 Schematic representation of *EWSR1-CREB1* fusions. Genomic rearrangements of *EWSR1-CREB1* were found in the four current cases. (a) A genomic breakpoint was found at 719 bp downstream of *EWSR1* exon 7 and 2967 bp upstream of *CREB1* exon 7, which leads to the generation of a fusion transcript that contains *EWSR1* exons 1–7 and *CREB* exons 7–9 (a, current Case 1). A genomic breakpoint was found at the exact 3' end of *EWSR1* exon 8 and 3809 bp upstream of *CREB1* exon 7, which was supposed to cause a fusion transcript that contains *EWSR1* exons 1–8 and *CREB1* exons 7–9. However, RNA NGS assay detected an unexpected transcript that skipped *EWSR1* exon 8 and only contains *EWSR1* exons 1–7 and *CREB1* exons 7–9 (b, current Case 2). A genomic breakpoint was found at 525 bp downstream of *EWSR1* exon 7 and 4028 bp upstream of *CREB1* exon 7, which leads to the generation of a fusion transcript that contains *EWSR1* exons 1–7 and *CREB* exons 7–9 (c, current Case 3). A genomic breakpoint was found at 854 bp downstream of *EWSR1* exon 7 and within *CREB1* exon 6 (35 bp to the 3' end of this exon), which leads to the generation of a fusion transcript that contains *EWSR1* exons 1–7 and *CREB* exons 6–9 (d, current Case 4).

Table 3 Clinicopathological characteristics of lung metastatic angiomatoid fibrous histiocytoma

| Case | Sex | Age (years) | Primary tumor size | Primary tumor site | Lung metastasis | Primary tumor morphology | Outcome | Survival | Reference |
|------|------|-------------|--------------------|-----------------------|------------------------|-----------------------------|---------|-------------------|---|
| M1 | Male | 21 | 50 mm | Supraclavicular | Massive tumor | NA | DOD | 13 years | Enzinger <i>et al.</i> (1979) ¹ |
| M2 | Male | 34 | NA | Left thigh | Multiple small lesions | NA | DOD | 18 months | Enzinger <i>et al.</i> (1979) ¹ |
| M3 | Male | 10 | 60 mm | Back subcutis | NA | Pleomorphic cells 20/10HPFs | DOD | 17 years 6 months | Matsumura <i>et al.</i> (2010) ⁹ |
| M4 | Male | 54 | 230 mm | Thigh skeletal muscle | NA | Pleomorphic cells 15/10HPFs | DOD | 1 year 3 months | Matsumura <i>et al.</i> (2010) ⁹ |
| M5 | NA | 3 | 60 mm | Neck | NA | NA | DOD | 21 months | Costa <i>et al.</i> (1995) ⁴⁴ |
| M6 | Male | 34 | 303 mm | Thigh, intramuscular | Multiple metastasis | AFH classic morphology | DOD | 4 years | Saito <i>et al.</i> (2017) ⁴⁵ |

DOD, died of disease; M, metastatic case; NA, no available data.

was very low (1%–3%). EWSR1 gene translocation was detected in all four cases (Fig 1i–l). However, neither ALK gene translocation nor CNV were observed in all of the cases.

Three fusion variants EWSR1-CREB1 (E7; C7), EWSR1-CREB1 (E8; C7), EWSR1-CREB1 (E7; C6) were detected in the four cases by NGS DNA level test (Table 2, Fig 2). One fusion variant which was EWSR1-CREB1 (E8; C7) on DNA level was found to produce EWSR1-CREB1 (E7; C7) transcripts in the NGS RNA assay (Fig 2b). This indicates the exon 8 of EWSR1 gene was skipped during RNA splicing procedure.

Prognosis

The prognosis data were available in all four cases, and the follow-up time was from 13 to 30 months. No regional lymph nodes or distant metastasis, recurrence and tumor-related death after resection were reported in all cases. The data are summarized in Table 1.

Discussion

AFH occurring in the subcutis of extremities and outside somatic soft tissue is referred to as classic somatic or unusual sites entities, respectively, and they show differences in clinicopathological features and prognosis.² PPAFH is very unusual, and only 10 PPAFH cases have been reviewed in the literature from seven published articles during 2009 to 2019.^{2,7,8,17–20} Combined with the four new cases in this study, all 14 cases are reviewed and summarized in Table 1. Clinical and pathological information is provided in 13 of 14 patients. There was a slight predilection for PPAFH to arise in males with eight males (61.5%) and five females (38.5%) whose mean and median age was 47.2 years and 49 years, respectively (range 22–70 years). There were two cases in the literature who presented with endotracheal masses with symptoms of dyspnea, stridor, or

acute respiratory failure, and five cases presented with endobronchial masses, with cough and sputum production, dyspnea on exertion or hemoptysis.^{17–19} No smoking history (0/5) was recorded. There were two cases who had suffered from pulmonary TB and one with breast carcinoma concurrently (literature Case 8).²⁰ One patient had been occupationally exposed to asbestos (literature Case 5).¹⁹ In total, seven of 13 cases presented with a polypoid mass or a nodule located in the endotrachea or bronchus. Tumor sizes ranged from 1.3 to 8.0 cm, and the average and median size was 2.2 and 1.5 cm, respectively. The most common histological features of PPAFH included delineated or partial hyaline fibrous capsule (100%, 13/13), lymphoplasmacytic cuff (92.3%, 12/13), dense or richly lymphoplasmatic infiltration (100%, 13/13). Pseudo-angiomatous spaces were uncommon (33.3%, 3/9). Focal nuclei pleomorphic were evident in six of 12 cases. Mitoses were present in up to 3/10 HPF in three cases. No necrosis was identified in all cases. There were nine of 10 cases who presented with focal to obvious myxoid change with reticular pattern, focal sclerotic stroma (four cases) or hemorrhage. In comparison with nonpulmonary unusual sites and classic AFH, PPAFH cases showed the greater mean age (PPAFH 49 years vs. nonpulmonary unusual sites 27 years vs. classic AFH 13 years) and the age of all of PPAFH cases was above 20 years, with smaller tumor size (PPAFH 1.5 cm vs. nonpulmonary unusual sites 3.8 cm vs. classic AFH 2–2.8 cm). There was also less frequency of pseudoangiomatous spaces (33.3%, 3/9) in morphology.

The etiology was unclear and no special condition was associated with PPAFH. In consideration of somatic AFH occurring as second tumors or with infection condition,^{21,22} one PPAFH case had been occupationally exposed to asbestos and two had longstanding TB, and long-term pulmonary chronic inflammation or injury may therefore be a potential risk factor for PPAFH.

Among the 14 PPAFH patients, seven cases were recorded to have an endotracheal or bronchial mass. The tumor location related with large airway is a distinctive feature for PPAFH and should be included in the differential diagnostic criteria for pulmonary metastatic AFH and other mesenchymal tumors. Morphologically, hyaline fibrous capsule, lymphoplasmacytic cuff and dense or richly lymphoplasmatic infiltration are the most frequent morphological changes in PPAFH cases, and pseudoangiomatous spaces in lesions are less common than that of somatic AFH.²³ Same as somatic sites and nonpulmonary AFH counterparts, diversified and heterogeneous morphological changes are also one of the features of PPAFH.

Regarding IHC stains, the diffuse membranous patterns of epithelial membrane antigen (EMA) were observed in eight cases (61.5%, 8/13). Desmin was positive in seven cases with dendritic pattern (53.8%, 7/13). CD163 or CD68 was positive in nine cases (81.8%, 9/11). SMA was found focal positive in five cases (38.5%, 5/13). Using Ventana ALK (D5F3) kit detecting ALK protein expression was observed in 3/4 current cases, take together ALK expression was observed 5/7 cases (71.4%). Cytokeratin (AE1/AE3), CD21, CD23 and CD35 was negative in tumor cells. Positive expression of TLE1 was observed in the four current cases. EMA, desmin, CD68 or CD163, ALK, and TLE1 expression are the most common positive IHC markers for PPAFH diagnosis. ALK expression was observed in 5/7 cases,^{8,24} and it is a pitfall that PPAFH might be misdiagnosed to be a pulmonary ALKoma tumor,^{25,26} especially inflammatory myofibroblastic tumor (IMTs) in the lung; on the other hand, it becomes one of the common IHC biomarkers for diagnosis of PPAFH. Recently, SOX9 and MUC4 was verified to be positive in AFH cases and suggested as useful markers for PPAFH differential diagnosis.^{27,28}

Molecular tests are considered to be crucial for the diagnosis of AFH, and three kinds of gene translocation changes have been previously reported in AFH cases: EWSR1-CREB1, EWSR1-ATF1 and FUS-ATF1 gene fusion.^{29,30} 13/13 PPAFH cases showed EWSR1 gene rearrangement and 62.5% (5/8) with EWSR1-CREB1 and 37.5% (3/8) with EWSR1-ATF1; no FUS-ATF1 was found in all of the PPAFH cases. Pulmonary primary mesenchymal tumors harboring EWSR1 gene rearrangements include PPAFH, PPMS, myoepithelial tumors, hyalinizing clear cell carcinoma (HCCC), extraskeletal myxoid chondrosarcoma (EMC), and clear cell sarcoma, etc. However, the fusion partners may be different. For example, EWSR1-POU5F1, EWSR1-PBX1 and EWSR1-ZNF444 are common fusion variants in myoepithelial tumors, and 93% of HCCC cases showed EWSR1-ATF1 fusion. EWSR1-NR4A3 is a frequent fusion variant in EMC.^{31,32} To ascertain the partner genes and whether the molecular pathways in which EWSR1

is involved has a value in differential diagnosis, it may be more promising to use NGS, especially an RNA-based NGS technique, in the clinical tests for the differential diagnosis of pulmonary mesenchymal tumors.

The prognostic data were available in eight cases, the median follow-up time was 23 months from 13 to 150 months (the first reported PPAFH case was followed-up by phone call in the current study [the follow-up was approved by the Institutional Review Board of Air Force Medical Center of PLA]). No cases of recurrence, distant metastasis or tumor-related death after resections were recorded. Only one case (literature Case 8) presented with mediastinal lymph node metastasis which was verified by surgical resection sample and the medical history suggested that the patient may be an immunocompromised individual (with longstanding TB and a history of breast cancer).

The morphological features and molecular alterations of PPAFH overlaps with wide spectrum pulmonary mesenchymal tumors. For IMTs, the mesenchymal tumor has been reported to represent 0.04%–0.1% of pulmonary primary tumors and account for 20% of primary pulmonary neoplasms in pediatric patients.^{10,33} In a previous study, the prevalence of pulmonary primary IMTs has been reported to be much higher than PPAFH, patients with IMTs have been reported to be younger in age (mean) than in those patients with PPAFH, and the average tumor size larger than that of PPAFH (4.5 vs. 2.2 cm).³³ In a previous study, PPAFH presented as a well circumscribed tumor, but 21% of pulmonary primary IMTs were found to involve adjacent structures.³³ Albeit predominant spindle cell tumor and intratumor lymphoplasmatic infiltration is seen in both entities, but the other characteristic morphological features and heterogeneous morphological components of PPAFH are not seen in IMTs. ALK expression can be seen in both, but the molecular alterations are totally different.^{34–36} However, it has also been previously reported that whilst both tumors have an excellent prognosis, 17% of patients with pulmonary IMTs presented with metastasis and one case died of disease.³³

PPMS was coined by Thway *et al.*¹¹ and in the World Health Organization (WHO) classification of lung tumors it is included as a distinct tumor, although PPAFH and PPMS has significant overlap in clinicopathological, morphological and molecular features and is considered as a continuum spectrum in morphology and biology.^{37–41} Comparing the latest case report with the literature reviewing 26 PPMS cases,⁴² the average tumor size of PPMS was greater than that of PPAFH (4 vs. 2.2 cm), and most PPMS cases presented as a myxoid tumor with predominant myxoid stroma, but just focal and up to 30% myxoid stroma was reported in PPAFH cases. Mild to severe atypia and focal necrosis was recorded in PPMS cases, but just mild atypia of tumor cells

and no necrosis were described in PPAFH cases. The distinctive histological changes of AFH (even in the myxoid variant AFH)⁴³ such as fibrous pseudocapsule, lymphoplasmacytic infiltration and fibrous sclerosis were present in both, but much more frequently in PPAFH than in PPSM and no peritumor lymphoplasmacytic cuff was described in PPSM. With regard to IHC, CD68 or CD163, Desmin, EMA and ALK positive expression, PPAFH should be considered, but not PPSM. It is 100% (13/13) PPAFH cases harboring EWSR1 rearrangement and 79% in PPSM, and 37.5% (3/8) PPAFH patients with the EWSR1-ATF1 variant, but very few in PPSM cases. In a recent study, three PPSM cases presented with distant metastasis, one had metastasized to the brain and died of disease,⁴⁰ but no recurrence, distant metastasis and death from disease were recorded in PPAFH cases.

In patients with AFH, pulmonary metastasis should also be taken into consideration for a differential diagnosis from PPAFH. As in our review, six classic site AFH cases were reported to have lung metastasis after primary tumor resections and local recurrences, which followed an extremely aggressive outcome, and all six cases died of disease. However, no pulmonary metastatic AFH clinicopathological features overlapped with PPAFH.^{9,44,45} The clinicopathological characteristics of lung metastatic angiomatoid fibrous histiocytoma are reviewed and summarized in Table 3.

In conclusion, PPAFH is very rare but has distinctive clinicopathological features. Combined with the clinicopathological features, IHC staining results, and molecular alterations test, an algorithm for the differential diagnosis of pulmonary primary mesenchymal spindle cell tumors is recommended. First, observe the tumor location, PPAFH, PPSM, IMT and salivary gland-type tumors which may present as an endobronchial tumor or have a relationship with the large airways. Second, determine if the morphological features, well-circumscribed, fibrous capsule, lymphoplasmacytic cuff, dense or richly lymphoplasmatic infiltration are PPAFH morphological features. Third, whilst there are no specific immunoprofiles for a definite differential diagnosis, CK, EMA, desmin, SMA, CD68 or CD163, CD99, S100, P63, calponin, and dendritic cell markers are recommended for a definitive diagnosis of PPAFH. Finally, FISH for *EWSR1* and *ALK* gene rearrangement test, and RNA-based NGS are powerful auxiliary tools to secure a differential diagnosis.

Acknowledgments

Guiping Han, Chunyan Wu and Dongge Liu designed the study and wrote the paper; Zheng Wang, Liping Zhang, Li Ren performed study for collecting pulmonary primary angiomatoid fibrous histiocytoma cases with clinical data, reviewing histological slides and wrote the paper; Du Jun,

Ge Lou contributed FISH test and results analysis; Min Zhang analyzed the radiology images; Ying Song, Yin Wang performed the next generation sequencing test; We thank Jing Di and Li Yang for their contribution in technical support, Fei Gai for support in submission.

Disclosure

No authors report any conflict of interest.

References

- Enzinger FM. Angiomatoid malignant fibrous histiocytoma: A distinct fibrohistiocytic tumor of children and young adults simulating a vascular neoplasm. *Cancer* 1979; **44**(6): 2147–57.
- Chen G, Folpe AL, Colby TV *et al.* Angiomatoid fibrous histiocytoma: Unusual sites and unusual morphology. *Mod Pathol* 2011; **24**: 1560–70.
- Slack JC, Sanchez-Glanville C, Steele M, Wong AL, Brundler MA. Retroperitoneal angiomatoid fibrous histiocytoma presenting as a recurrent spontaneous retroperitoneal hemorrhage in a 9-year-old boy. *J Pediatr Hematol Oncol* 2018; **40**: 307–11.
- Ghigna MR, Hamdi S, Petitpretz P *et al.* Angiomatoid fibrous histiocytoma of the pulmonary artery: A multidisciplinary discussion. *Histopathology* 2014; **65**: 278–82.
- Mangham DC, Williams A, Lalam RK, Brundler MA, Leahy MG, Cool WP. Angiomatoid fibrous histiocytoma of bone: A calcifying sclerosing variant mimicking osteosarcoma. *Am J Surg Pathol* 2010; **34**: 279–85.
- Spatz M, Nussbaum ES, Lyons L, Greenberg S, Kallmes KM, Nussbaum LA. Primary intracranial angiomatoid fibrous histiocytoma: A case report and literature review. *Br J Neurosurg* 2018; **15**: 1–3.
- Ren L, Guo SP, Zhou XG, Chan JK. Angiomatoid fibrous histiocytoma: First report of primary pulmonary origin. *Am J Surg Pathol* 2009; **33**: 1570–4.
- Cheah AL, Zou Y, Lanigan C *et al.* ALK expression in angiomatoid fibrous histiocytoma: A potential diagnostic pitfall. *Am J Surg Pathol* 2019; **43**: 93–101.
- Matsumura T, Yamaguchi T, Tochigi N, Wada T, Yamashita T, Hasegawa T. Angiomatoid fibrous histiocytoma including cases with pleomorphic features analysed by fluorescence in situ hybridisation. *J Clin Pathol* 2010; **63**: 124–8.
- Khatri A, Agrawal A, Sikachi RR, Mehta D, Sahni S, Meena N. Inflammatory myofibroblastic tumor of the lung. *Adv Respir Med* 2018; **86**: 27–35.
- Thway K, Nicholson AG, Lawson K *et al.* Primary pulmonary myxoid sarcoma with EWSR1-CREB1 fusion: A new tumor entity. *Am J Surg Pathol* 2011; **35**: 1722–32.

- 12 Zhu L, Li J, Liu C *et al.* Pulmonary inflammatory myofibroblastic tumor versus IgG4-related inflammatory pseudotumor: Differential diagnosis based on a case series. *J Thorac Dis* 2017; **9**: 598–609.
- 13 Denning KL, Olson PR, Maley RH Jr, Flati VR, Myers JL, Silverman JF. Primary pulmonary follicular dendritic cell neoplasm: A case report and review of the literature. *Arch Pathol Lab Med* 2009; **133**: 643–7.
- 14 Salido M, Pijuan L, Martinez-Aviles L *et al.* Increased ALK gene copy number and amplification are frequent in non-small cell lung cancer. *J Thorac Oncol* 2011; **6**: 21–7.
- 15 Roehr JT, Dieterich C, Reinert K. Flexbar 3.0 - SIMD and multicore parallelization. *Bioinformatics* 2017; **33**: 2941–2.
- 16 Li H, Durbin R. Fast and accurate short read alignment with burrows-wheeler transform. *Bioinformatics* 2009; **25**: 1754–60.
- 17 Chen W, Shi H, Liu Y, Ke Z, Han A. Endotracheal angiomatoid ‘malignant’ fibrous histiocytoma: EWSR1 gene rearrangement. *Pathology* 2013; **45**: 506–8.
- 18 Bouma W, Koning KJ, Suurmeijer AJH, Slebos DJ, Mariani MA, Klinkenberg TJ. Hybrid bronchoscopic and surgical resection of endotracheal angiomatoid fibrous histiocytoma. *J Cardiothorac Surg* 2019; **14**: 48.
- 19 Thway K, Nicholson AG, Wallace WA, Al-Nafussi A, Pilling J, Fisher C. Endobronchial pulmonary angiomatoid fibrous histiocytoma: Two cases with EWSR1-CREB1 and EWSR1-ATF1 fusions. *Am J Surg Pathol* 2012; **36**: 883–8.
- 20 Tay CK, Koh MS, Takano A, Aubry MC, Sukov WR, Folpe AL. Primary angiomatoid fibrous histiocytoma of the lung with mediastinal lymph node metastasis. *Hum Pathol* 2016; **58**: 134–7.
- 21 Gambini C, Haupt R, Rongioletti F. Angiomatoid (malignant) fibrous histiocytoma as a second tumour in a child with neuroblastoma. *Br J Dermatol* 2000; **142**: 537–9.
- 22 Pettinato G, Manivel JC, De Rosa G, Petrella G, Jaszcz W. Angiomatoid malignant fibrous histiocytoma: Cytologic, immunohistochemical, ultrastructural, and flow cytometric study of 20 cases. *Mod Pathol* 1990; **3**: 479–87.
- 23 Kao YC, Lan J, Tai HC *et al.* Angiomatoid fibrous histiocytoma: Clinicopathological and molecular characterisation with emphasis on variant histomorphology. *J Clin Pathol* 2014; **67**: 210–5.
- 24 Van Zwam P, Mentzel T, Flucke U. ALK expression in angiomatoid fibrous histiocytoma: Confirmation of the findings of Cheah *et al.* *Am J Surg Pathol* 2019; **43**: 1156.
- 25 Mano H. ALKoma: A cancer subtype with a shared target. *Cancer Discov* 2012; **2**: 495–502.
- 26 Osoegawa A, Nosaki K, Miyamoto H *et al.* Incidentally proven pulmonary “ALKoma”. *Intern Med* 2010; **49**: 603–6.
- 27 Berklite L, John I, Ranganathan S, Parafioriti A, Alaggio R. SOX9 immunohistochemistry in the distinction of angiomatoid fibrous histiocytoma from histologic mimics: Diagnostic utility and pitfalls. *Appl Immunohistochem Mol Morphol* 2020; **28**: 635–40.
- 28 Abrahao-Machado LF, Bacchi LM, Fernandes IL, Costa FD, Bacchi CE. MUC4 expression in angiomatoid fibrous histiocytoma. *Appl Immunohistochem Mol Morphol* 2020; **28**: 641–5.
- 29 Thway K, Fisher C. Angiomatoid fibrous histiocytoma: The current status of pathology and genetics. *Arch Pathol Lab Med* 2015; **139**: 674–82.
- 30 Tanas MR, Rubin BP, Montgomery EA *et al.* Utility of FISH in the diagnosis of angiomatoid fibrous histiocytoma: A series of 18 cases. *Mod Pathol* 2010; **23**: 93–7.
- 31 Thway K, Fisher C. Mesenchymal tumors with EWSR1 gene rearrangements. *Surg Pathol Clin* 2019; **12**: 165–90.
- 32 Jeffus SK, Gardner JM, Steliga MA, Shah AA, Stelow EB, Arnaoutakis K. Hyalinizing clear cell carcinoma of the lung: Case report and review of the literature. *Am J Clin Pathol* 2017; **148**: 73–80.
- 33 Weldon CB, Shamberger RC. Pediatric pulmonary tumors: Primary and metastatic. *Semin Pediatr Surg* 2008; **17**: 17–29.
- 34 Cessna MH, Zhou H, Sanger WG *et al.* Expression of ALK1 and p80 in inflammatory myofibroblastic tumor and its mesenchymal mimics: A study of 135 cases. *Mod Pathol* 2002; **15**: 931–8.
- 35 Lovly CM, Gupta A, Lipson D *et al.* Inflammatory myofibroblastic tumors harbor multiple potentially actionable kinase fusions. *Cancer Discov* 2014; **4**: 889–95.
- 36 Kazmierczak B, Dal Cin P, Sciort R, Van den Berghe H, Bullerdiek J. Inflammatory myofibroblastic tumor with HMGIC rearrangement. *Cancer Genet Cytogenet* 1999; **112**: 156–60.
- 37 Travis WD, Brambilla E, Burke AP, Marx A, Nicholson AG. *WHO Classification of Tumours of the Lung, Pleura, Thymus and Heart.*, 4th ed. Lyon, France: ARC Press 2015; 9–148.
- 38 Koelsche C, Tavernar L, Neumann O *et al.* Primary pulmonary myxoid sarcoma with an unusual gene fusion between exon 7 of EWSR1 and exon 5 of CREB1. *Virchows Arch* 2019; **476**: 787–91.
- 39 Kim S, Song SY, Yun JS, Choi YD, Na KJ. Primary pulmonary myxoid sarcoma located in interlobar fissure without parenchymal invasion. *Thorac Cancer* 2017; **8**: 535–8.
- 40 Prieto-Granada CN, Ganim RB, Zhang L, Antonescu C, Mueller J. Primary pulmonary myxoid sarcoma: A newly described entity-report of a case and review of the literature. *Int J Surg Pathol* 2017; **25**: 518–25.
- 41 Smith SC, Palanisamy N, Betz BL *et al.* At the intersection of primary pulmonary myxoid sarcoma and pulmonary angiomatoid fibrous histiocytoma: Observations from three new cases. *Histopathology* 2014; **65**: 144–6.
- 42 Chen Z, Yang Y, Chen R, Ng CS, Shi H. Primary pulmonary myxoid sarcoma with EWSR1-CREB1 fusion: A case report and review of the literature. *Diagn Pathol* 2020; **15**: 15.

- 43 Schaefer IM, Fletcher CD. Myxoid variant of so-called angiomatoid "malignant fibrous histiocytoma": Clinicopathologic characterization in a series of 21 cases. *Am J Surg Pathol* 2014; **38**: 816–23.
- 44 Costa MJ, McGlothlen L, Pierce M, Munn R, Vogt PJ. Angiomatoid features in fibrohistiocytic sarcomas. Immunohistochemical, ultrastructural, and clinical distinction from vascular neoplasms. *Arch Pathol Lab Med*. 1995; **119**(11):1065–71.
- 45 Saito K, Kobayashi E, Yoshida A *et al.* Angiomatoid fibrous histiocytoma: A series of seven cases including genetically confirmed aggressive cases and a literature review. *BMC Musculoskelet Disord* 2017; **18**: 31–5.